Thermal Convection in a Rotating Fluid Annulus: Part 3. Suppression of the Frictional Constraint on Lateral Boundaries

GARETH P. WILLIAMS

Geophysical Fluid Dynamics Laboratory, ESSA, Washington, D. C.[1]

(Manuscript received 5 February 1968, in revised form 7 May 1968)

ABSTRACT

In certain rotating fluid systems such as the atmosphere, the flow must maintain a zero net torque on the horizontal surface. The character of such flows is sought through numerical integration of the Navier-Stokes equations. The fluid occupies a torus shaped region whose vertical boundaries are assumed to be frictionless. The solutions relate to either a laboratory annulus with hypothetical free-slip sidewalls or to a zonal strip of the atmosphere or ocean. All the solutions are qualitatively similar despite parametric differences; their flows have a westerly-easterly zonal wind distribution near the horizontal boundary together with direct and indirect cells in a manner reminiscent of that proposed by classical theory for the general circulation of the atmosphere.

Under a strong external temperature differential the isotherms concentrate into a front. The meridional circulation assumes the form of gliding motion parallel to the front together with frictionally driven secondary circulations. Certain mesoscale geophysical phenomena also possess these characteristics.

The solutions provide good examples of Eliassen's theory of vortex circulations.

1. Introduction

This paper forms the third part of a study of the axisymmetric thermal convection of a fluid contained in a rotating, annular-shaped region (Fig. 1). The cylinders which form the lateral boundaries are assumed to be frictionless, only the horizontal base having a frictional interaction with the fluid. Solutions of strongly convective flows are obtained by numerical integration of the Navier-Stokes equations. We shall apply the solutions on 1) the laboratory scale, to make a study of the effect of the sidewall frictional layers on convection in the annulus, and 2) on the larger geophysical scale, to examine the role of rotational and thermal forces in determining the features of large-scale convective phenomena such as the general circulation, fronts and squall lines.

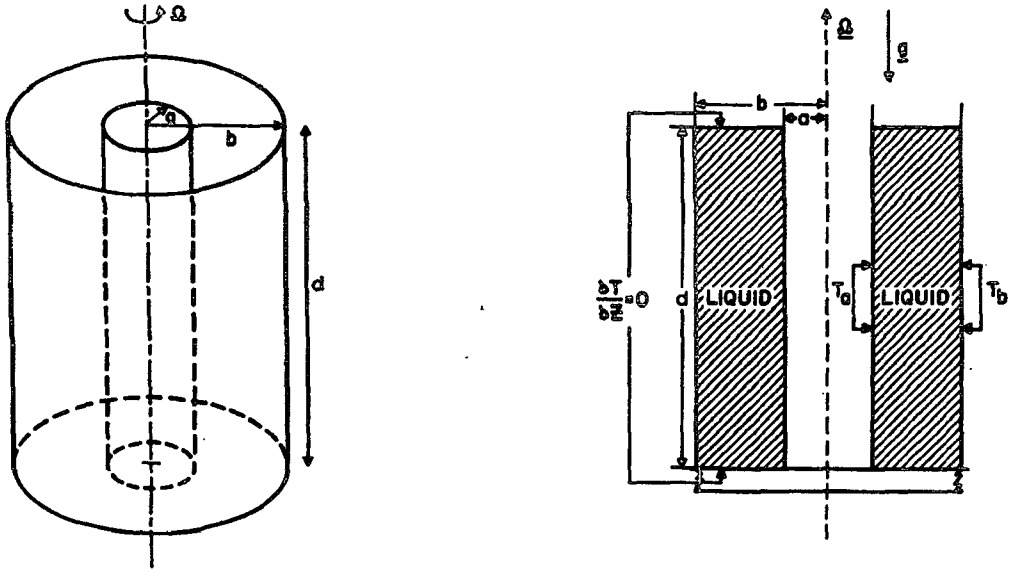

FIG. 1. The physical configuration for which solutions are obtained. The diagram on the left shows the geometry and that on the right the physical condition of the system.

[1] Now: Geophysical Fluid Dynamics Laboratory/ESSA, Princeton University, Box 308, Princeton, N. J. 08540.

Laboratory annulus flow is often said to be analogous to the general circulation of the atmosphere. However, this statement is not specific enough and the analogy must be strictly defined. We know from McIntyre (1968) and Williams (1967a,b) that the frictional and thermal sidewall boundary layers play a dominant role in shaping the real annulus flow. The meridional velocity and temperature fields are largely boundary layer phenomena and, therefore, these fields cannot be analogous to any geophysical counterpart. On the other hand, the zonal velocity has only a very weak direct coupling with the meridional motion and it is essentially produced as a forced, geostrophic response to the separately determined temperature field. This situation resembles certain theoretical states such as that assumed for baroclinic instability theory, where the response of the zonal velocity to a fixed temperature field is examined, as shown, for example, by Eady (1949). Thus, the only close analogy in the axisymmetric state lies in the *geostrophy* of the zonal motions (rather than in the motion itself). To demonstrate the importance of the boundary layers on the cylinder walls in determining the flow of the laboratory annulus, solutions for systems with both frictional and frictionless lateral boundaries will be presented. The solutions differ radically. The hypothetical annulus with its free-slip lateral boundaries possesses meridional fields that are not controlled by boundary layers and so have a greater overall analogy to geophysical flows. We will use this analogy of meridional velocity, temperature and zonal velocity to investigate some aspects of the nature of the general circulation and mesoscale flows.

One problem to be examined concerns the general circulation of the atmosphere. Classical theories of the general circulation were constructed around the basis of longitudinal symmetry, with large-scale eddies being assumed to play a minor disturbing role. Hadley, Ferrel, Oberbeck, Kropatschek and others proposed axisymmetric meridional cell systems to account for limited observations [see Lorenz (1967) for an interesting review of these theories]. More extensive observation repudiated these explanations. However, it remains an interesting hypothetical question as to what steady-state axisymmetric motion could exist in an atmosphere with neither zonal asymmetries nor disturbances. This question also arises in general circulation calculations (Manabe *et al.*, 1965), in which the initial integrations assume a zonal symmetry to produce a rapid development to a baroclinically unstable condition. A simple Hadley cell with easterly winds at the surface predominates over the first 90 days. At this stage baroclinic instability is allowed to develop and produce zonal asymmetries. We suspect that had the symmetric integration been continued, the flow existing at 90 days would not prevail in the equilibrium state where angular momentum balance must occur. Yet we do not know what type of circulation would arise. It is hoped that solutions of the hypothetical system, while not directly applicable, will indicate the general type of motion that can exist under similarly located heat and momentum sources.

The importance of vertical motions in forming and maintaining the structure of such medium-scale phenomena as fronts, squall lines and thunderstorms has been acknowledged and stressed by many writers. Past studies of atmospheric fronts showed that the intensification of the temperature gradient was initiated by deformation of the horizontal wind field. More recent studies (Eliassen, 1959) indicate that completion and maintenance of the front is accomplished by deformation of the vertical wind field. Theoretical analyses have been mainly qualitative and always based on an assumed existence of the frontal concentration. However, under appropriate values of the Rossby and Taylor parameters, solutions exhibiting strong frontal-like temperature concentrations can be produced within the annular zone. Thus, the solutions will be used to produce and examine the flow structure in frontal zones. The front is assumed to be in steady-state equilibrium and have similarly located heat and momentum sources to those of the real atmosphere; the precise mechanism for the heat sources is not the same, however, only their effect.

From a more general viewpoint, the solutions can be regarded as providing examples of strongly nonlinear convective flow in a rotating vortex. It is hoped that a variety of such solutions would lead to a greater familiarity with nonlinear, medium Rossby-number flows and provide a quantitative base for such analytical studies as Eliassen's (1952) theory for thermally controlled meridional circulations in a circular vortex. The numerical solutions agree with the heuristic analysis of Eliassen (1952) for general convective flow, for the general circulation between equator and mid-latitudes, and with his 1959 analysis of frontal flow.

2. Equations of axisymmetric transfer

We consider a fluid bounded by two co-axial cylinders of inner and outer radii a, b, respectively, and two parallel horizontal planes which are a distance d apart, (Fig. 1). The container rotates at a constant rate Ω, where the rotation vector coincides with the vertical axis of the cylinders. Motion is considered relative to the solid rotation and is measured in cylindrical coordinates r, z based on the axis, r being radial and z vertical. The variables u, v, w denote velocity components in the zonal, radial and vertical directions. The inner and outer lateral boundaries are held at different constant temperatures T_a and T_b, respectively ($T_b > T_a$). This imposed horizontal temperature differential, $\Delta T = T_b - T_a$, drives the fluid away from a state of solid rotation. The base ($z=0$) and upper surface ($z=d$) are thermally insulating, i.e., $T_z = 0$.

Referring to Williams (1967 a), hereafter denoted by Part 1, for greater detail, the equations for axisymmetric

TABLE 1. Composition of cases computed.* The system has free-slip lateral boundaries and upper surface, and a non-slip base. The outer and inner sidewalls are held at constant temperatures, $\bar{T}+(\Delta T/2)$, $\bar{T}-(\Delta T/2)$, respectively. The base and surface are insulated.

Case	Number of given intervals in r, z	a (cm)	b (cm)	d (cm)	ΔT (°C)	Ω (rad sec^{-1})	π_4**	π_5**	Ro†	Nū†
A3B	40×60	3.48	6.02	5.0	29.0	1.342	2.510	1.5×10^{6}	0.9267	4.00
A4	40×40	3.0	6.0	3.0	5.0	0.4	2.090	5.1×10^{5}	0.9567	3.90
A5	60×40	5.0	20.0	5.0	10.0	0.1	4.470	5.98×10^{7}	5.334	31.5

* Constants: $\nu=1.008\times10^{-2}$ cm^2 sec^{-1}, $\kappa=1.42\times10^{-3}$ cm^2 sec^{-1}, $\beta=2.05\times10^{-4}$ (°C)$^{-1}$, $\bar{T}=20$C, $g=981.0$ cm sec^{-2}.
** $\pi_4\equiv(g\beta\Delta Td)/[\Omega^2(b-a)^2]$, $\pi_5\equiv[4\Omega^2(b-a)^5]/(\nu^2 d)$.
† Rossby and Nusselt numbers given by solution and are defined by: $\mathrm{Ro}\equiv U_{\max}/(a\Omega)$, $\mathrm{N\bar{u}}\equiv\frac{1}{2d}\log\left(\frac{b}{a}\right)\int_0^d[a\theta_r(a)+b\theta_r(b)]dz$.

flow under the Boussinesq approximation may be written as follows:

$$\zeta_t+J\left(\psi,\frac{\zeta}{r}\right)=-\beta gT_r+2u_z\left(\Omega+\frac{u}{r}\right)+\nu\left\{\zeta_{zz}+\left[\frac{1}{r}(r\zeta)_r\right]_r\right\}, \quad (1)$$

$$u_t+\frac{1}{r}J(\psi,u)=\frac{1}{r}\psi_z\left(2\Omega+\frac{u}{r}\right)+\nu\left\{u_{zz}+\left[\frac{1}{r}(ru)_r\right]_r\right\}, \quad (2)$$

$$T_t+\frac{1}{r}J(\psi,T)=\kappa\left[T_{zz}+\frac{1}{r}(rT_r)_r\right], \quad (3)$$

$$\frac{1}{r}\psi_{zz}+\left(\frac{1}{r}\psi_r\right)_r=-\zeta, \quad (4)$$

$$m_t+\frac{1}{r}J(\psi,m)=\nu\left[m_{zz}+r\left(\frac{1}{r}m_r\right)_r\right], \quad (5)$$

$$m\equiv r(u+\Omega r), \quad (6)$$

where $J(\psi,\ )\equiv\psi_r(\ )_z-\psi_z(\ )_r$ represents the convection term. The stream function ψ and vorticity ζ describe the flow in the vertical r, z plane and are defined by

$$rv=-\psi_z,\ rw=\psi_r,\ \zeta=v_z-w_r. \quad (7)$$

Eq. (5) for the absolute angular momentum m is given for convenient reference.

The upper surface and lateral boundaries are assumed to be free-slip surfaces; thus, the tangential stresses and normal velocities at these boundaries must vanish. The base forms the only rigid boundary and here both tangential and normal velocities must vanish. Apart from new slip conditions that require the tangential stresses to vanish on the lateral boundaries, i.e., $\zeta=0$ and $(u/r)_r=0$, the equations and boundary conditions resemble those of Part 1.

Solutions of these equations can be obtained by making minor modifications to the numerical scheme given in Part 1. Although the equations were originally set up to describe the so-called annulus experiments, alteration of the boundary conditions allows us to consider their behavior in the broader context of convection in a general rotating system.

3. Parameter range of computations

Solutions were obtained for the three sets of parameter values, denoted as A3B, A4 and A5, shown in Table 1. Flows under these parameter values are strongly influenced by convective and rotational processes, as indicated by Rossby numbers of order 1. The stability of the flows remains unknown.

To compare flow under free-slip sidewalls with that under rigid sidewalls, a solution to free-slip case A3B was obtained. A3B has the same parameter values as the known solution, A3, for real annulus flow, given in Part 1. Cases A3B and A3 differ only in the dynamical condition on the lateral boundaries and a comparison illustrates the role of sidewall friction layers in determining flow.

The solutions for cases A4, A5 and A3B describe flow over a wide range of parameter conditions and illustrate, in particular, the variation due to geometrical factors; case A5 considers the flow in a wide annular gap (compared to height), whereas case A3B examines flow in a narrow annulus. The annulus in A4 has a gap width equal to its height. The cases were constructed to show that over this parameter range all flows have the same intrinsic structure.

4. Description of computed flows

The procedure for computing the solutions of the hypothetical annulus flows resembles the method described for the real annulus flow in Part 1. Starting from an initial condition of solid rotation, integration to a steady state was made for the three cases. We present these steady-state solutions in this section.

A uniform finite difference grid best resolves the strong interior and boundary gradients produced during the computation. The solutions indicate that the resolution (Table 1) does not suffice fully only in the case A5. The inadequacy occurs near the lateral boundaries and is a consequence of the relatively large horizontal dimension of the A5 annulus. This large dimen-

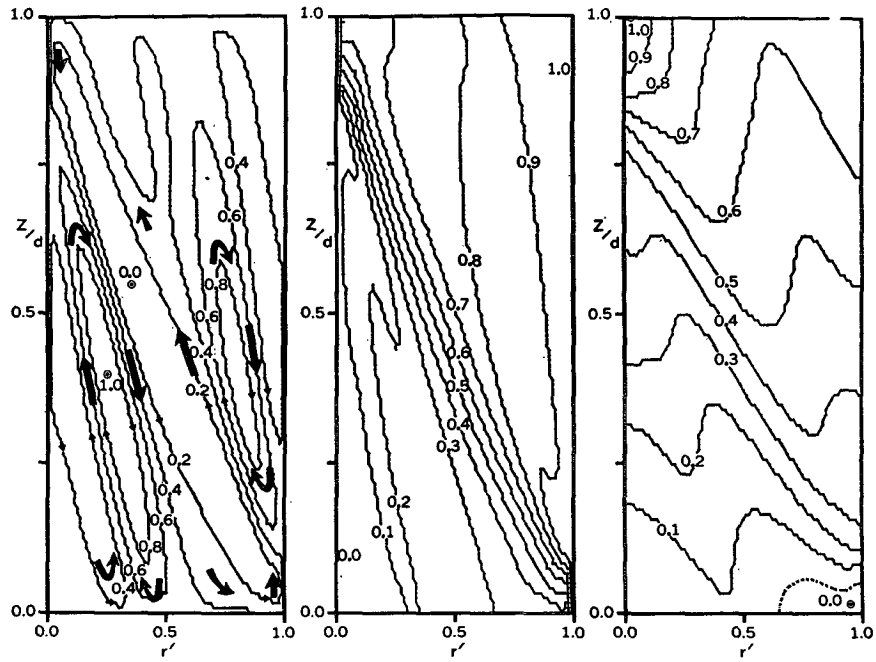

FIG. 2. The steady-state contours, from left to right, of stream function, temperature and zonal velocity for flow A3B (see Table 1). Each variable is normalized with respect to its maximum and minimum values. The normalized maximum and minimum have the respective values of 1.0 and 0.0; other contours are shown at intervals of 0.1 or 0.2. The absolute value of ψ, for example, may be determined from the equation $\psi=\psi_{\min}+$contour value$\times(\psi_{\max}-\psi_{\min})$, where the absolute maximum and minimum values are $+0.1607$, -0.1180 cm^3 sec^{-1} for ψ; 34.5, 5.5C for T; and $+4.328$, -0.1272 cm sec^{-1} for u. Stream function arrows indicate direction of meridional flow and positive zonal velocity indicates flow in the direction of the rotation (westerly). A dotted line indicates the zero line of zonal flow below which flow is easterly. The non-dimensional radial coordinate $r'\equiv(r-a)/(b-a)$ commences at the cold inner cylinder (on left of each graph).

sion also caused the flow to take a substantially longer time to reach a steady state than did the other flows. Case A3B approaches the limit of validity of the Boussinesq approximation (Part 1).

a. Flow features of case A3B

Fig. 2 illustrates the steady-state contours of the A3B solution. The temperature field concentrates into a frontal-like layer, lying diagonally from the top of the cold inner boundary to the bottom of the hot outer boundary. Outside the frontal layer, the temperature distributes itself uniformly except for a region around the 0.1 and 0.2 isotherms near the base. Here a secondary temperature concentration appears. The slopes of the two fronts differ.

The meridional flow takes place in three strong and two weak closed circulations. The main cell lies along the primary front, the upflow branch coinciding with the 0.7 isotherm and the downflow branch with the 0.3 isotherm. Flow across the temperature layer occurs only at its extremities. This circulation is in the nature of a sloping Hadley, or direct circulation, cell. The two cells adjacent to the Hadley cell have so-called indirect circulations, the lower, stronger cell touching the base. Two further direct circulations fill the space between the indirect (Ferrel) cells and the boundaries; these circulations are very weak as can be gaged from the relative areas of the velocity profiles of Fig. 3. The secondary temperature concentration occurs where the lower Ferrel cell interacts with the weak Hadley cell of the inner boundary.

The fluid mainly flows in the same sense as the rotation, i.e., westerly, but has enough of an easterly component along the outer half of the base to provide a zero net torque on the base. The zonal velocity reaches a maximum near the top of the inner boundary and a minimum near the bottom of the outer boundary; both extremes are associated with the temperature front.

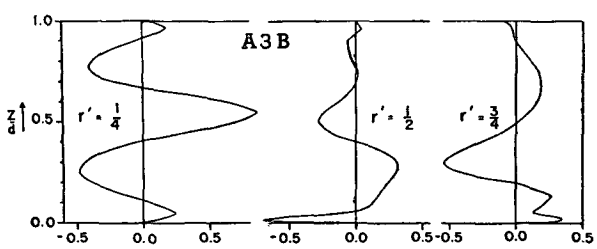

FIG. 3. Vertical distribution of radial velocity for A3B. Values are in mm sec^{-1} for planes $r'=\frac{1}{4}$, $\frac{1}{2}$, $\frac{3}{4}$ between the lateral boundaries.

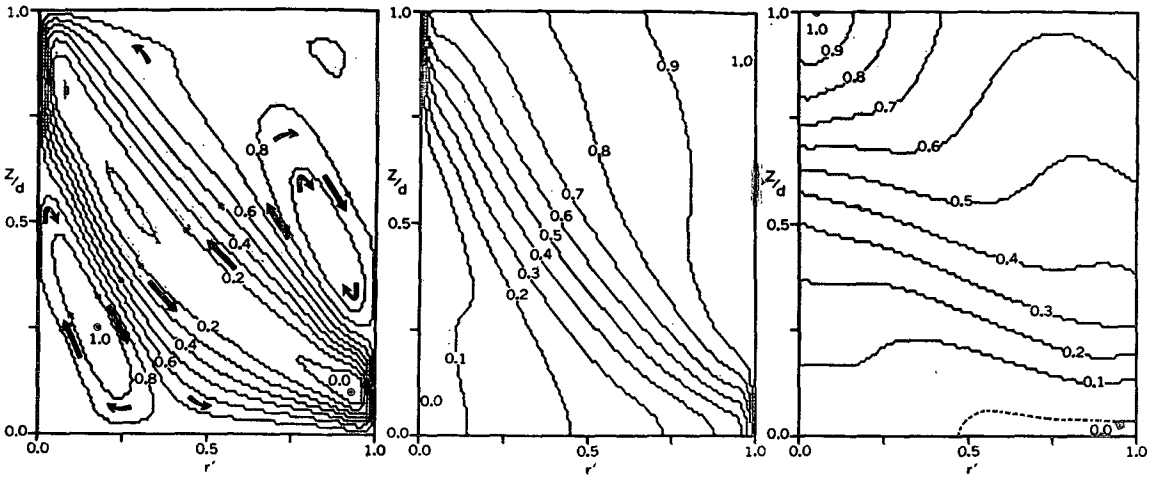

FIG. 4. The steady-state normalized contours of stream function, temperature and zonal velocity for flow A4. The absolute maximum and minimum values are +0.01478, −0.05147 cm³ sec⁻¹ for ψ; 22.5, 17.5C for T; and +1.148, −0.0058 cm sec⁻¹ for u.

The zonal isotachs lie parallel to the isotherms over a major part of the diagonal region, reflecting the highly convective nature of the flow.

The transient development (not shown) of the A3B flow from an initial state of solid rotation reveals a similarity to the evolution of the A3 flow of Fig. 14, Part 1, up to the 31.5-sec stage. At this instant the flow leaves the lateral boundaries as there is insufficient friction to maintain strong layers. The main circulation then proceeds to orientate itself about the diagonal and the indirect cells appear. During this phase the isotherms develop from a uniform distribution into the concentrated band of Fig. 2.

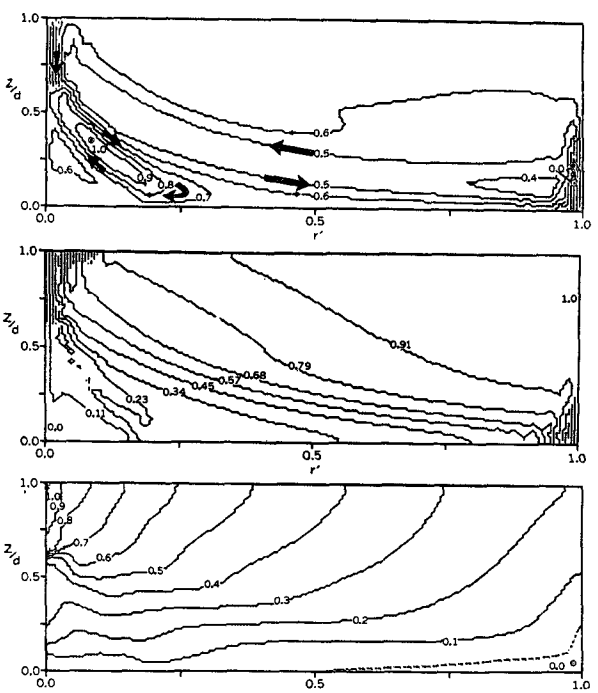

FIG. 5. The steady-state normalized contours of stream function, temperature and zonal velocity for flow A5. The absolute maximum and minimum values are +0.5351, −1.105 cm³ sec⁻¹ for ψ; 25, 15C for T; and +2.667, −0.05955 cm sec⁻¹ for u.

b. Flow features of cases A4 and A5

The solutions for two strongly convective flows A4, A5 in different shaped regions are shown in Figs. 4 and 5, respectively. In both cases a direct (Hadley) cell sloping along a layer of isotherms forms the main meridional circulation. The temperature contours lie near the diagonal region but do not concentrate as strongly as in the A3B solution. The geometrical factors or the higher temperature differential or both could be responsible for producing the stronger concentration in the A3B solution. Two indirect cells form the secondary circulation of A4, whereas A5 has no discernible circulation above the main Hadley cell, only an indirect cell below it. A second concentration of temperature appears in A5 at the intersection of the Ferrel cell and the very weak Hadley cell of the inner lateral boundary.

Thermal and vorticity boundary layers occupy small regions in the three solutions. The unevenness of the stream function and temperature contours of A5 indicates that the solution to this flow has inadequate resolution in the boundary regions and as a consequence lacks accuracy.

Westerly flow dominates the zonal velocity field. The peak value occurs near the top of the inner boundary and again sufficient easterly flow takes place, near the outer part of the base, to yield the necessary zero net torque and angular momentum balance.

c. Component balances

As the three solutions display similar characteristics, the component terms of only one case, A3B, will be presented. Figs. 6, 7 and 8 display representative radial

distributions of the component terms of the equations determining the steady state flow A3B.

A geostrophic balance between the Coriolis term $2\Omega u_z$ and the buoyancy term $-\beta g T_r$ dominates the components of the vorticity equation (Fig. 6). However, both these terms are small in the upper and outer part of the fluid. The nonlinear term $(u^2/r)_z$ plays an appreciable role in modifying this geostrophic balance in the region of the westerly maximum. The convection term $-J(\psi,\zeta,r)$ contributes little and the frictional force $\nu\{\zeta_{zz}+[1/r(r\zeta)_r]_r\}$ becomes significant in the interior only in areas where cells interact. This frictional force balances the strong buoyancy force at the top of the inner boundary and bottom of the outer boundary to produce vorticity boundary layers. These small layers compare in size with the thermal boundary layers.

The components of the zonal velocity equation given in Fig. 7 clearly show the intense convective nature of the flow. The two individual constituents of the zonal velocity convective term exceed their sum total by an order of magnitude. The Coriolis and viscous terms, although smaller, are important in some regions.

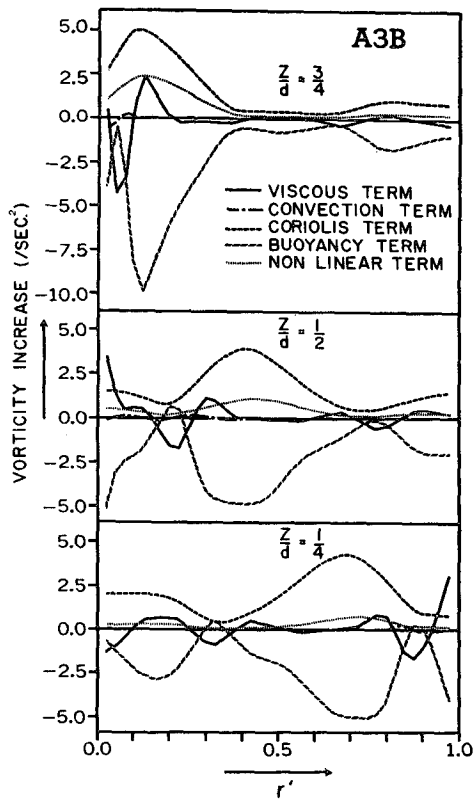

FIG. 6. Characteristic radial distributions (to within one grid-point of the boundary) of the balanced component terms of the vorticity equation, for steady-state flow A3B. Terms shown at heights $d/4$, $d/2$, $3d/4$ are (i) viscous: $\nu\{\zeta_{zz}+[1/r(r\zeta)_r]_r\}$, (ii) convection: $-J(\psi, \zeta/r)$, (iii) Coriolis: $2\Omega u_z$, (iv) buoyancy: $-\beta g T_r$, and (v) nonlinear: $(u^2/r)_z$. Individual viscous and convection components being of the same order as their respective totals are not shown separately. Graph indicates a geostrophic balance.

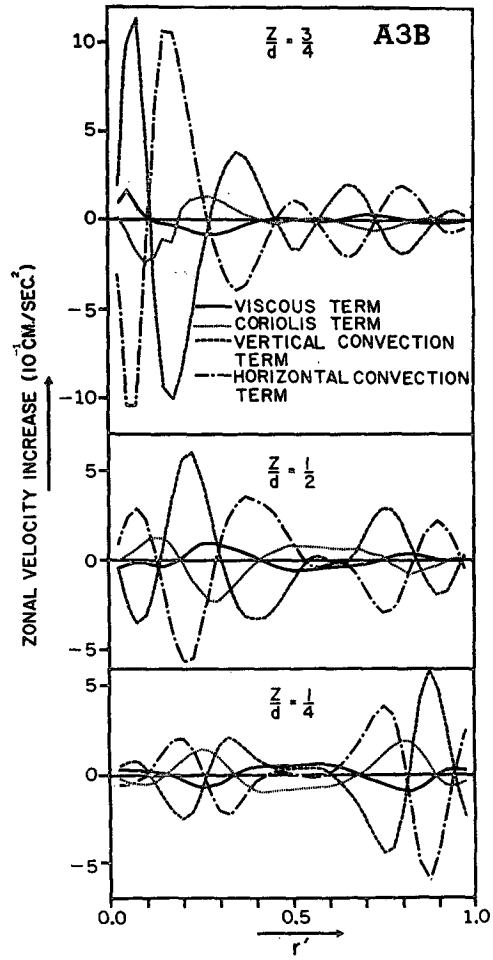

FIG. 7. Characteristic radial distributions (to within one grid point of the boundary) of the balanced component terms of the zonal velocity equation, for steady-state flow A3B. Terms shown at heights $d/4$, $d/2$, $3d/4$ are (i) viscous: $\nu\{u_{zz}+[1/r(ru)_r]_r\}$, (ii) horizontal convection: $-1/r(rvu)_r$, (iii) vertical convection: $-(wu)_z$ and (iv) Coriolis: $(2\Omega+u/r)(-v)$. Individual viscous components are not shown separately as they are of the same order as the total term.

Convective processes also dominate the component balance of the temperature equation shown in Fig. 9. The conduction process contributes only to the balance of isolated regions at an extremity of the lateral boundaries. We need consider only the total conduction term as the individual components of the term are of the same order as the sum total.

A notable feature of the A3B flow is the apparently linear form of the isotherms in the frontal region. The above component balances indicate that the conduction of heat is a negligible transport mechanism in this region. Under this circumstance the steady state form of the temperature equation can be written as

$$\frac{T_r}{T_z}=\frac{\psi_r}{\psi_z}, \tag{8}$$

which implies that the slopes of the T and ψ contours

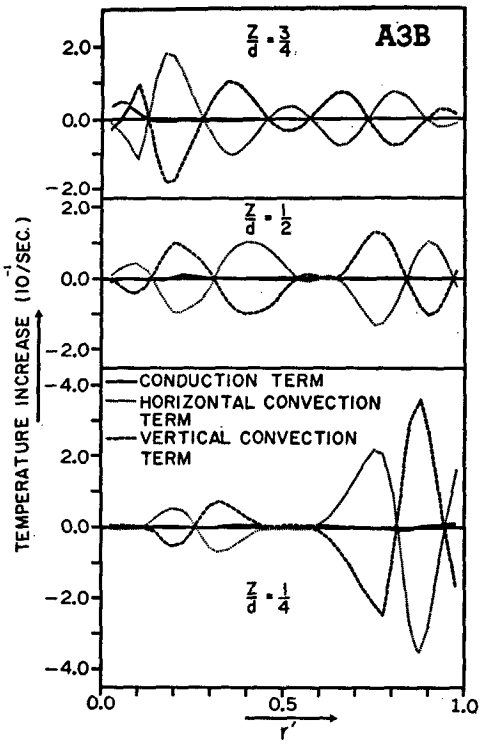

FIG. 8. Characteristic radial distributions (to within one grid point of the boundary) of the balanced component terms of the temperature equation, for steady state flow A3B. Terms shown at heights $d/4$, $d/2$, $3d/4$ are (i) conduction: $\kappa[T_{zz}+1/r(rT_r)_r]$, (ii) horizontal convection: $-1/r(rvT)_r$ and (iii) vertical convection: $-(wT)_z$. Individual conduction terms are not shown separately as they are of the same order as the total term.

are locally equal. In the A3B solution the T and ψ contours are parallel over much of the flow. Values of T_r/T_z and rT_r/T_z for the 0.5 contour of A3B, lying wholly within the front, are given in Table 2. Clearly, the values of rT_r/T_z vary little, particularly in the central part, so that we can write

$$rT_r/T_z = \text{a constant}, \tag{9}$$

for the frontal region. Thus, the frontal slope actually varies as r^{-1} and is not linear as appearances suggest.

5. Theoretical interpretation of the numerical solutions

In this section we will try to provide an explanation for the existence of the flows and interpret the flow structure in terms of the mechanics. At present the only relevant tool available to help explain such solutions is the theory due to Eliassen (1952) for slow thermally or frictionally controlled meridional circulation in a circular vortex. We will show that the solutions are consistent with Eliassen's theory and make use of his conclusions in examining the flow structure. For convenience the discussion is confined to the A3B solution.

TABLE 2. Values of the ratio of the radial to vertical gradient of temperature for the 0.5 temperature contour of the A3B solution.

r'	r	T_r/T_z	rT_r/T_z
0.175	3.92	2.62	10.28
0.325	4.31	2.28	9.81
0.525	4.81	2.05	9.88
0.675	5.19	1.78	9.25
0.800	5.51	1.61	8.86

The relative magnitudes of the component terms (Figs. 6–8) indicate the essential convective nature of the flows, so that, to a good approximation, the governing equations may be written

$$\frac{1}{r}J(\psi,T)=\mathrm{H}, \tag{10}$$

$$\frac{1}{r}J(\psi,m)=G, \tag{11}$$

$$\beta g T_r=\frac{\Omega}{r}2m_z, \tag{12}$$

where the conduction H is zero except in the corner regions of the thermal boundary layers and the friction effect G is zero except in the Ekman layer on the base and in the regions of cell interaction. These equations combine into a single equation for the stream function, namely,

$$[A\psi_r+B\psi_z]_r+[B\psi_r+C\psi_z]_z=\beta g H_r-\frac{\Omega}{r}2G_z, \tag{13}$$

where

$$A\equiv\frac{g}{r}\beta T_z, \quad B\equiv-\frac{g}{r}\beta T_r\left(=-\frac{\Omega}{r^2}2m_z\right), \quad C\equiv\frac{\Omega}{r}2m_r. \tag{14}$$

The parameters A, B and C are measures of the static stability, baroclinicity and inertial stability, respectively.

Eq. (13) resembles that deduced by Eliassen (1952) for slow thermally or frictionally controlled meridional circulation in a circular vortex. Eliassen used this equation to examine the general circulation of the atmosphere and later (1959, 1962) to investigate the vertical circulation in frontal zones.

For the conclusions of Eliassen's theory to be applicable to the A3B solution, Eq. (13) must be of an elliptic, or generalized Poisson, type. The condition for ellipticity is that the discriminant δ of the equation, defined by

$$\delta^2=AC-B^2=\frac{\Omega}{r^2}2\beta g(T_z m_r-T_r m_z), \tag{15}$$

be greater than zero. This requirement is met if the m contours are more vertical than the T contours; this is so, particularly in the frontal layer (cf. Figs. 2 and 9).

Using (13), Eliassen (1952) examined the circulations caused by point sources of heat and angular mo-

mentum. He found that a point source of heat produces two elliptic shaped cells, one on each side of the source, having streamlines that run through the point source at a tangent to an m line through the source. For a point source of angular momentum, a similar cell system occurs except that now the streamlines run through the source at a tangent to a constant T line through the source. The sense of the circulation is such that motion is away from the axis of rotation through an angular momentum source and is toward the axis through a sink. When the angular momentum source lies on a boundary the flow pattern is made up of a single elliptical cell with streamlines through the source, all touching the boundary. The linearity of the theory allows the resulting circulation of multiple sources to be obtained simply by adding the motions caused by each separate effect.

Applying these theoretical results, we see that the solution A3B can be considered as having one heat source and one heat sink, not quite point sources but small enough to apply the theory. The main Hadley cell is associated with both source and sink. The streamlines tend to go through the source-sink regions but these regions lie at the intersection of two bounding surfaces which greatly modify the simple cell structure of Eliassen's theory. The heat source and sink act together to produce the strong central circulation.

A source of angular momentum exists whenever $\nu[m_{zz}+r(m_r/r)_r]$ is significantly positive. In the solutions, source regions occur on the outer half of the base and at the interaction of the main direct cell and lower indirect cell (for A3B: $z'=0.5$, $r'=0.4$). Angular momentum sinks arise where the lower indirect cell meets the base (for A3B: $r'=0.45$); a sink of similar magnitude forms where the main cell and upper indirect cell interact near the outer boundary (for A3B: $z'=0.25$, $r'=0.8$). The region of highest zonal velocities forms the third angular momentum sink. The reader may find it helpful to refer to a composite ψ, m diagram (Fig. 11) drawn up by Eliassen (1952) for the atmospheric circulation (to be discussed in Section 7), but which also provides a partial schematic illustration of the heat and momentum sources of the solutions.

While these angular momentum sources are not point sources, they are sufficiently localized for Eliassen's deductions to apply. All the circulations are consistent in position, shape and direction with those that would be expected to occur by the theoretical results for such angular momentum sources and sinks. For example, the lower indirect cell is consistent with the action of the angular momentum source at the interaction with the Hadley cell and with the angular momentum sink at the base. As there are no heat sources acting on this cell, we may conclude that it is frictionally driven. The main cell, being subject to both heat and angular momentum sources, forms a more complex structure.

As far as the overall structure of flows such as A3B is concerned, the above cell structures imply that the

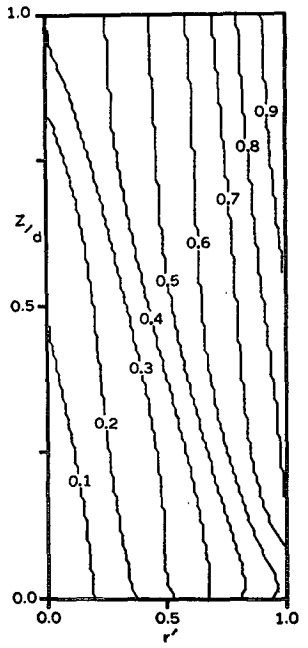

FIG. 9. The steady-state contours of absolute angular momentum for flow A3B. The absolute maximum and minimum values of m are 66.14, 16.25 cm^2 sec^{-1}.

flow is basically driven by being heated near the bottom of the outer boundary and cooled near the top of the inner boundary. The main circulation, extending from the heat source to heat sink, carries angular momentum from its main source in the surface easterlies into the upper westerlies near the inner boundary. This supply of angular momentum maintains the zonal velocity against frictional dissipation. The lower indirect cell receives angular momentum from the main cell by friction and loses it to the base in the zone of surface westerlies. The upper indirect cell (A3B, A4) loses angular momentum to the main cell through frictional action. The angular momentum sinks in the westerly maximum, Ekman layer, and upper indirect cell all compare with each other in magnitude.

The convergence, at the base, of meridional flow from the indirect cell and from the weak inner direct cell creates the secondary front defined by the 0.1 and 0.2 isotherms of A3B and A5. This front can thus be said to have been induced by the frictional action of the main Hadley cell.

The above description accounts for the distribution and maintenance of the angular momentum and meridional velocity for the existing temperature field, in a manner consistent with the sources and sinks of angular momentum and heat. However, explanations of why such a temperature field evolves in preference to any other and of why the heat sources concentrate into small areas, are not obvious.

It should be recognized that the above explanation, by its use of Eliassen's theory, in effect takes the friction and conduction effects to be known forcing functions.

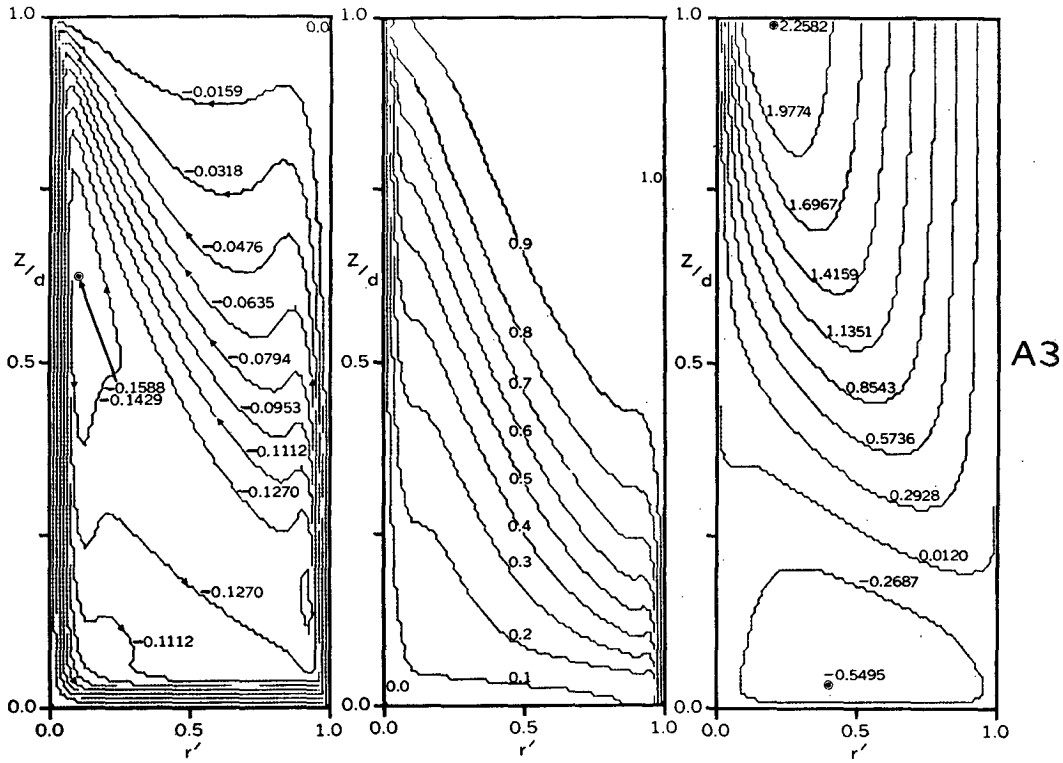

FIG. 10. The steady-state contours of the stream function, normalized temperature and zonal velocity for the rigid lateral boundary flow A3 (Part 1). Compare with free-slip flow A3B which has identical parameter values.

A more satisfactory explanation is needed in which reasons for the existence of the heat and angular momentum sources is also established.

6. Implication of the solutions for laboratory flows

In this section we shall consider the solutions described above from the viewpoint of laboratory-scale flow. Principal concern will be with comparing the two solutions A3B and A3; the latter was presented in Part 1 but the contours are reproduced in Fig. 10 for convenience.

The two flows differ both qualitatively and quantitatively. The meridional circulations reflect 1), the dominance of the boundary layers in forming the meridional velocities of real annulus flow (A3), and 2), the highly convective nature of flow freed from the necessity of maintaining boundary layers (A3B).

The temperature fields have a similar orientation about the diagonal but with A3B having the more intense concentration. The Nusselt numbers of the heat transfer, 4.00 and 8.14 for A3B and A3, respectively, reveal the efficiency of boundary layers as heat transporters.

The zonal velocities are similar in the sense that both maxima occur in the same region and that values increase with height. The maximum value for the flow A3B is almost double that for the real annulus flow A3. The easterlies of A3B occupy only a small area and are much weaker.

Although the component terms exhibit different meridional balances, both flows are essentially geostrophic. However, in A3B a strong nonlinear coupling between ψ and T,u supplements the geostrophic linking of u to T.

It is of some interest to note that the flow A4 under free-slip boundaries has a similar normalized temperature field to rigid flow A3, despite differences in geometric and other parameters.

7. Geophysical implication of solutions

The numerical solutions have some geophysical bearing if we accept the provisos 1) that the geophysical turbulent momentum and heat transports correspond to the laminar viscosity and conductivity formulation of the Navier-Stokes equations to a degree in keeping with the role of these processes in the overall system; 2) that the variation of Ω with latitude is a secondary effect and can be neglected; 3) that the atmospheric potential temperature corresponds to the temperature variable of the solutions; 4) that the annulus base and upper surface be analogous to the earth's surface and tropopause, respectively; and 5) that $T_z=0$ is the boundary condition on both surfaces. The causes of heating are not related and only established temperature fields can be dealt with.

Many atmospheric phenomena exist under and are maintained by the influence of rotation and a temperature differential. The solutions may be relevant to such phenomena because the dominant scaling parameters, the Rossby and Taylor numbers, have similar values.

a. The general circulation of the atmosphere

If we take the outer and inner lateral boundaries of the solutions to represent the equator and some middle latitude zone below the jet stream, respectively, then solution A5 may describe, approximately, the axisymmetric circulation within that region. Eliassen (1952) has suggested that the atmospheric circulation should be of the form depicted in Fig. 11.

In formulating a theory for the symmetric general circulation, the choice of an appropriate heating system remains ambiguous because of the hypothetical nature of such a flow. In the situation shown in Fig. 11, air is supposed to be heated in low levels near the equator; the release of latent heat in the up-flow branch of the indirect cell generates another heat source. Sinks of heat due to excess radiation in warm, subsiding air occur, supposedly, at about 40N.

Solution A5 (Fig. 5) bears a particular resemblance to the above scheme; unlike the other solutions it has no upper indirect cell and so has a strict one-to-one correspondence of all angular momentum sources and sinks. Equatorial heat sources are equivalent, but in higher latitudes the solution possesses a single upper level heat sink whose position differs slightly to that derived by crude estimates for the atmosphere. No analogy exists between the natures of the heating mechanisms, but from the dynamical aspect only identical location of the heating sources and sinks really matters.

The flows depicted in Fig. 5 (for A5) and Fig. 11 (for the atmosphere) imply an atmosphere with a meridional circulation consisting of two main cells. The large thermally driven Hadley cell extends from the earth's surface at the equator to the upper west wind maximum in middle latitudes. The smaller indirect frontal (Ferrel) cell receives angular momentum and energy from the Hadley cell through friction and loses angular momentum to the ground in the zone of surface westerlies. The front associated with the Ferrel cell occurs along the up-flow branch of the circulation; in Fig. 5 the 0.11 and 0.23 isotherms outline the front. The meridional streamlines run mainly parallel to the isentropes.

The description of the angular momentum balance given in Section 5 for the solutions applies also to the above atmospheric circulation. The multiple cell configuration appears to be necessary to satisfy the condition, met by solution A5, that there is no net torque on the earth, i.e., an angular momentum balance exists.

b. Fronts and squall lines

The existence of a strong temperature concentration in solution A3B leads us to examine the relevance of this

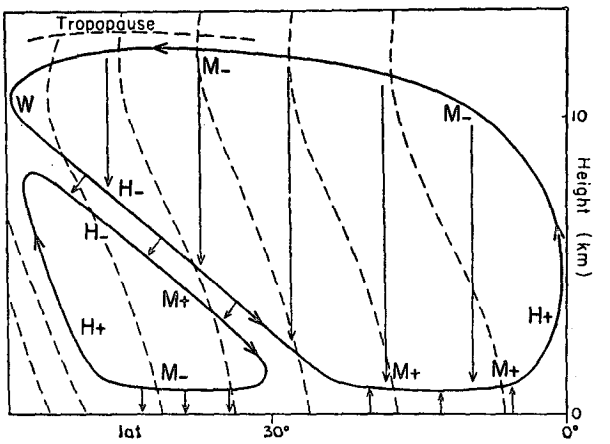

FIG. 11. Schematic meridional circulation system of the atmosphere, proposed by Eliassen (1952); diagram after Väisänen (1961). Thin dashed lines are lines of constant angular momentum (cf Fig. 9). Solid lines are meridional streamlines. Arrows indicate turbulent transfer of angular momentum. $M_+(M_-)$ indicate sources (sinks) of angular momentum, and $H_+(H_-)$ sources (sinks) of heat. There are surface easterlies in latitudes 0° to 30° and surface westerlies from 30° northward to 45°.

solution to atmospheric frontal systems. To compare the solution to the atmosphere the following assumptions must be accepted: 1) that the front is quasi-stationary and has reached a steady-state equilibrium; 2) that the lateral boundaries correspond to the boundaries of a mid-latitude zone in which curvature effects do not play a crucial part; and 3) that condensation processes are not an essential ingredient for frontal formation—fronts have been observed in the ocean and dishpan (Faller, 1956; Fultz, 1952) so the condition is probably not restrictive. With these assumptions the solution describes the flow that takes place in the layer between two fluid masses of infinite heat capacity, one boundary being at a much higher temperature than the other. No mixing is allowed between the enclosed layer and the bounding masses so the interaction is somewhat artificial.

Solution A3B indicates that a sloping front forms between the two bounding masses, with cold fluid wedged beneath the warm. Of the many cells associated with the front, the main direct cell takes the form of a gliding movement along both sides of the front. Heat enters the system at the leading edge of the front and leaves at the top of the rear edge, thermal conduction between the layer and boundaries bringing about both transfers. The frictionally induced indirect cell produces a secondary front.

The solution and atmospheric situation differ in one important respect; namely, the strong meridional flow across the front in the solution may be modified in the atmosphere by inflow from the boundary. The artificial suppression of inflow limits the comparison.

Despite the above differences, the frontal flow predicted by the solution agrees, in general, with that estimated for the atmosphere by Eliassen (1959, 1962); the

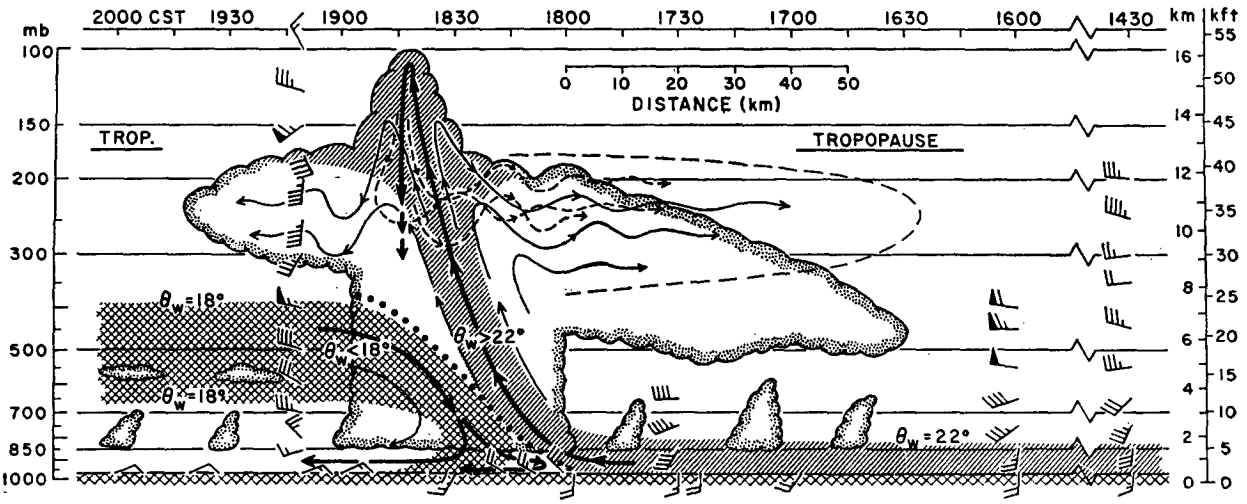

FIG. 12. Partly schematic cross section through a squall line (after Newton, 1966). Hatching indicates air with a temperature in excess of 22C ahead the squall line and its probable extent in the updraft. Cross hatching indicates extent of air of temperature below 18C.

physical configuration and governing equations are also similar. According to these equations and their analysis given in Section 5, convective processes determine the meridional circulation of frontal flows but the zonal velocity still responds geostrophically. The nonlinearity of convective motion makes it difficult to state why the front occurs. The concentration of heat source and sink into small areas in the solution has also been observed in squall lines, but it is not clear if this is the cause or effect of fronts.

Squall lines are a two-dimensional frontal phenomenon. The observations of Newton (1966) given in Fig. 12 display the estimated flow pattern and heat transport of a typical squall line; the figure bears a definite resemblance to solutions A3B and A4. In Fig. 12, a sloping cell constitutes the main motion within the storm; cloud distributions suggest the existence of secondary cell systems. The heat source occupies a small area at the leading edge of the storm. The cloud system supposedly exposes the downdraft of the main cell, subjecting it to cooling and gravitational sinking; this heat sink coincides with that of A3B. The combination of heating and cooling gives the squall line a great efficiency as an overturning process and makes the system the same as that of the solution despite different boundary constraints.

8. Conclusion

The flows considered appear to fall into a general category. The requirement of zero torque on the base produces multi-cell flows of the same character for three sets of parameter values, i.e., a main direct Hadley cell together with one or two indirect Ferrel cells. A westerly zonal flow predominates throughout the fluid except for a small region of weak easterly flow near the outer half of the base. Such flows occur over a wide range in the values of the parameters Ω, ΔT, a, b and d. For a large temperature differential and narrow zone, the temperature lines concentrate into frontal-like features but the basic pattern remains qualitatively the same as for the other flows.

The front arises in a flow exhibiting a strong convection of heat and angular momentum but maintaining geostrophy; in this state the temperature contours exhibit a linear or r^{-1} variation.

Analogies exist between the solutions and certain general circulation and frontal flows. This suggests that these two atmospheric phenomena are flows of the same dynamical type under different parameter values. Rather than form precise analogous systems for given heat and momentum sources, the solutions may be more relevant in showing what types of flow can occur under the influence of an Ekman layer and temperature differential. It may be more useful to know that strong frontal gradients can be produced from a neutral state than to specify how or by what process this production occurs.

The sidewall boundary layers play an intrinsic part in setting up and maintaining the flow in a real laboratory annulus. If these layers are ignored the resulting meridional flow is completely different and any theoretical analysis that does not allow for these layers is severely limited in its relevance to the real annulus.

Acknowledgments. The author is grateful to Drs. Kirk Bryan, Syukuro Manabe and Michael McIntyre for valuable comments and suggestions, and to Miss M. B. Jackson for preparing the figures.

REFERENCES

Eady, E. T., 1949: Long waves and cyclone waves. *Tellus*, **1**, 33–52.

Eliassen, A., 1952: Slow thermally or frictionally controlled meridional circulation in a circular vortex. *Astrophys. Norv.*, **5**, No. 2, 19–60.

——, 1959: On the formation of fronts in the atmosphere. *The Rossby Memorial Volume*, Rockefeller Institute and Oxford University, 277–287.

——, 1962: On the vertical circulation in frontal zones. *Geophys. Norv.* **24**, 147–160.

Faller, A., 1956: A demonstration of fronts and frontal waves in atmospheric models. *J. Meteor.*, **13**, 1–4.

Fultz, D. 1952: On the possibility of experimental models of the polar-front wave. *J. Meteor.*, **9**, 379–384.

Lorenz, E. N., 1967: The nature and theory of the general circulation. WMO Monogr. No. 218, TP. 115, 161 pp.

Manabe, S., *et al.*, 1965: Simulated climatology of a general circulation model with a hydrologic cycle. *Mon. Wea. Rev.*, **93**, 769–798.

McIntyre, M. E., 1968; The axi-symmetric convective regime for a rigidly-bounded rotating annulus. *J. Fluid Mech.*, **32**, 625–655.

Newton, C. W., 1966: Circulations in large sheared cumulonimbus. *Tellus*, **18**, 700–713.

Väisänen, A., 1961: A study of the symmetric general circulation by the aid of a rotating water tank experiment. *Geophysica*, **8**, 39–61.

Williams, G. P., 1967a: Thermal convection in a rotating fluid annulus: Part I. The basic axisymmetric flow. *J. Atmos. Sci.*, **24**, 144–161.

——, 1967b: Thermal convection in a rotating fluid annulus: Part 2. Classes of axisymmetric flow. *J. Atmos. Sci.*, **24**, 162–174.